

# MATERIAL SELECTION AND GEOMETRY CONSIDERATIONS FOR HIGH CURRENT SENSING MAGNETIC FLUX CONCENTRATOR DESIGNS

By Kevin Buckley  
Allegro MicroSystems

## INTRODUCTION

Many electrical and power systems require accurate current sensing measurements, e.g., traction motors, industrial automation, and electric vehicle chargers, just to name a few. Hall-effect based current sensors with integrated conductors are an ideal solution for these measurements, but as the current levels increase, the thermal capacity limits of the sensor will eventually be compromised. Most integrated conductor current sensors are only specified to operate at currents up to 50 A<sup>[1]</sup>, however, there are specialized packages that can handle up to 200 A<sup>[2]</sup>. For high accuracy, high current measurements beyond the thermal capability of integrated conductor current sensors it is common to use a magnetic flux concentrator, (also referred to in this note as a magnetic core), along with a Hall-effect current sensor.

The current carrying conductor is passed through the center of the magnetic flux concentrator which is fabricated with a ferromagnetic material, such as ferrite or other iron alloy. The magnetic field generated by the current in the conductor is focused in the magnetic core. An air gap is cut into the core, into which the Hall-effect sensor is placed perpendicular to the direction of the magnetic field. Figure 1 shows an example of a current sensing system using a flux concentrator with a Hall-effect sensor.

Core material selection, geometry, and air gap dimensions will all impact the performance of the flux concentrator. This note will explain each of these factors and provide a detailed guide for design of a magnetic flux concentrator.

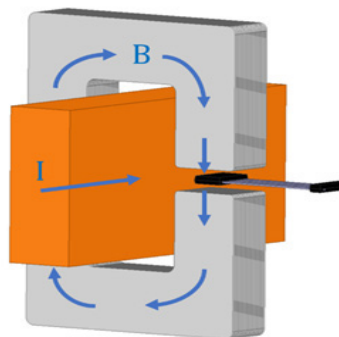


Figure 1: High Current Sensing System Using Magnetic Flux Concentrator

[1] Alex Latham and Scott Milne, "DC and Transient Current Capability/Fuse Characteristics of Surface Mount Current Sensor ICs", accessed August 6, 2021, <https://www.allegromicro.com/en/insights-and-innovations/technical-documents/hall-effect-sensor-ic-publications/dc-and-transient-current-capability-fuse-characteristics>

[2] Evan Shorman, Caleb Mattson, Shaun Milano, "DC Current Capability and Fuse Characteristics of Current Sensor ICs with 50 to 200 A Measurement Capability", accessed August 6, 2021, <https://www.allegromicro.com/en/insights-and-innovations/technical-documents/hall-effect-sensor-ic-publications/dc-current-capability-fuse-characteristics-current-sensor-ics-50-200-a>

## Flux Concentrator Material Selection

Magnetically soft materials, which can rapidly switch their magnetization in response to a magnetic field, are used in magnetic flux concentrator designs. Magnetic parameters critical to the performance of the concentrator are permeability, saturation magnetization, coercivity, and electrical conductivity. In designing a flux concentrator, the most important factors are achieving the highest saturation flux density with the lowest magnetic hysteresis (coercivity), while choosing a material with an acceptable cost. However, while optimizing one characteristic there are tradeoffs that must be considered. For example, the high saturation flux density and low cost of silicon iron (SiFe) may be attractive, but the lower hysteresis of nickel iron (NiFe) may be required to reduce measurement offsets at a significantly higher price point (>3×).

## Permeability

The permeability,  $\mu$ , is effectively a measure of how readily the core material responds to an applied magnetic field. Permeability is the magnetic equivalent of electrical conductance in an electric circuit. Magnetic materials with a high permeability will have low magnetic reluctance (analogous to electrical resistance) and are, therefore, more easily magnetized. A comparison of a flux concentrator to an electronic circuit is shown in Figure 2.

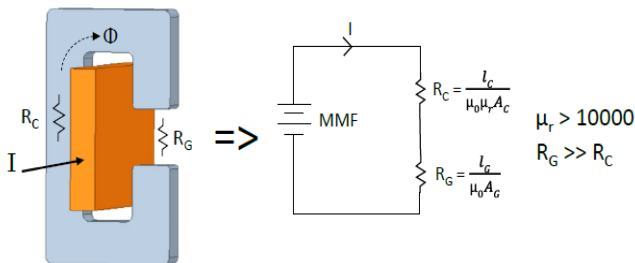


Figure 2: Electrical Representation of a Magnetic Circuit

In the equivalent electric circuit shown, the magnetomotive force created by the induced magnetic field in the magnetic circuit is replaced by a voltage source. The magnetic flux and reluctance of the core are analogous to the electric current and resistance in the electric circuit, respectively. The reluctance in the core is proportional to mean path length,  $l$ , and inversely proportional to permeability,  $\mu$ , and cross-sectional area,  $A$ . In a gapped core, the reluctance of the air gap will dominate the total reluctance of the core design and will dictate the amount of magnetic flux density being sensed by the current sensor placed in the air gap.

The permeability of the core material is important insofar as it is several orders of magnitude greater than the permeability

of air such that the air gap defines the magnetic coupling factor of the core. It is also important that the permeability of the material is stable over the operating temperature range. For example, permeability in ferrite cores can decrease rapidly at higher temperatures as shown in Figure 8.

## Saturation Magnetization

The saturation magnetization of a material is the point at which any increase in applied magnetic field no longer results in an increase in magnetic flux induced in the core. Driving the core into saturation could cause excessive hysteresis and will introduce non-linearities in the current measurement. Selecting a core material with a high saturation point and designing for magnetic flux densities below saturation levels is key to optimal performance. The relationship of saturation flux density vs permeability is shown for several iron alloys in Figure 3.

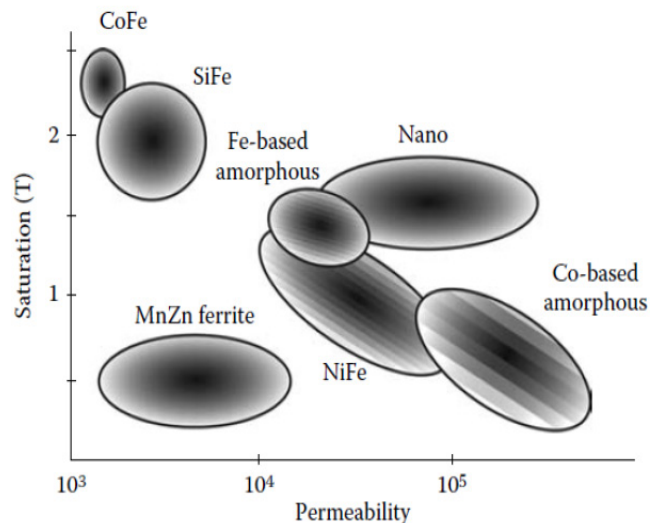


Figure 3: Saturation vs. Permeability in Iron Alloys [3]

## Coercivity (Magnetic Hysteresis)

The coercivity is a measure of the intensity of the applied magnetic field required to reduce the magnetic field to zero following magnetization of the core. The higher the coercivity of a magnetic material, the higher the magnetic hysteresis, which results in a residual B field when the current in the conductor is taken away or reversed. This will cause offsets in the current sensor measurements. Hysteresis is also a contributor to core losses at higher frequencies. For these reasons, the coercivity of the magnetic material must be taken into consideration. Figure 4 illustrates the relationship between material coercivity, saturation flux density, as well as cost.

[3] S. Tumanski. 23 Jun 2011, Magnetic Materials from: Handbook of Magnetic Measurements CRC Press

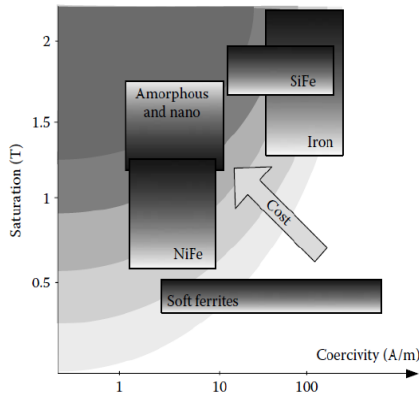


Figure 4: Saturation Flux Density vs Coercivity [4]

While NiFe has much lower hysteresis than SiFe, it also has lower saturation density and it can cost significantly more than SiFe. Figure 5 shows hysteresis curves for typical cores made of NiFe (78 Permalloy: 78% nickel, 22% iron) and SiFe (4% silicon, 96% iron). The NiFe has 10 × better hysteresis performance at ~60% saturation magnetization and, on average, ~3 × the cost.

It is important to understand how much hysteresis is acceptable in a core design to determine whether the extra cost of NiFe is required. Measurements taken on various SiFe open loop concentrator cores show that the current measurement offset error induced by the hysteresis is typically ±2 A regardless of core geometry and air gap dimensions [5]. For high current measurements of >200 A this error will be <1%.

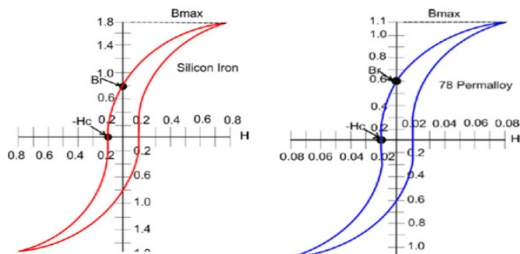


Figure 5: Hysteresis Curves for SiFe and NiFe Cores [6]

More detailed discussions regarding magnetic hysteresis and its impact on current sensing measurements can be found in detailed application notes on the Allegro Microsystems website [7][8].

[4] See note 3 above.

[5] Yannick Vuillermet and Loïc Messier, "Evaluation of Hysteresis Offset Error in Hall-Effect Current Sensors Using Soft Ferromagnetic Concentrator Cores", accessed August 6, 2021, <https://www.allegromicro.com/en/insights-and-innovations/technical-documents/hall-effect-sensor-ic-publications/hysteresis-mitigation-in-current-sensor-ics-using-ferromagnetic-cores>

[6] J.O. Aibangbee, O. Onohaebi, "Ferromagnetic Materials Characteristics: Their Application in Magnetic Cores design Using Hysteresis Loop Measurements", American Journal of Engineering Research, Volume-7, Issue-7, pp-113-119

[7] See note 5 above.

[8] Georges El Bacha, Shaun Milano, and Jeff Viola, "Hysteresis Mitigation in Current Sensor ICs Using Ferromagnetic Cores," accessed August 6, 2021, <https://www.allegromicro.com/en/insights-and-innovations/technical-documents/hall-effect-sensor-ic-publications/hysteresis-mitigation-in-current-sensor-ics-using-ferromagnetic-cores>

[9] Yannick Vuillermet, "High-Current Measurement with Allegro Current Sensor IC and Ferromagnetic Core: Impact of Eddy Currents," accessed August 6, 2021, [https://www.allegromicro.com/en/insights-and-innovations/technical-documents/hall-effect-sensor-ic-publications/an296162\\_a1367\\_current-sensor-eddy-current-core](https://www.allegromicro.com/en/insights-and-innovations/technical-documents/hall-effect-sensor-ic-publications/an296162_a1367_current-sensor-eddy-current-core)

## Electrical Conductivity

The electrical conductivity of the material selected will have a direct impact on the frequency response of the core. A core with low resistivity will be susceptible to eddy currents induced by a changing magnetic field. By Lenz's Law, eddy currents induced by the changing magnetic field will create their own magnetic field in opposition to the initial magnetic field as shown in Figure 6.

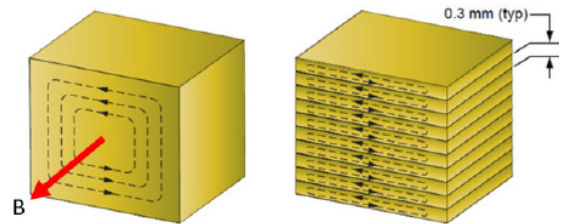


Figure 6: Eddy Currents in bulk material and laminated material

To minimize eddy currents iron alloys with higher resistivity, such as SiFe, are generally used. Additionally, the strength of the eddy current is proportional to the area of the current loop, so laminated cores manufactured with stacks of thin sheets of iron (or iron alloys) are used to minimize the area of the current loop and thus reduce the eddy current losses. Using thinner laminations will result in less core losses at higher frequencies due to eddy currents, as shown in Figure 7 for a core composed of SiFe sheets.

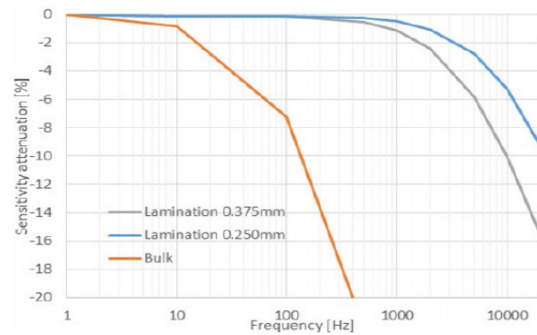


Figure 7: Core Sensitivity Attenuation vs Frequency vs Lamination Thickness [9]

## Temperature Stability

The ambient temperature range of the application must also be considered when selecting a core material. The permeability of the magnetic core will vary over temperature so a material with the appropriate temperature stability must be chosen for the system environment. As shown in Figure 8, the relative permeability of ferrite cores drops off sharply at higher temperatures making them unsuitable for applications that need to operate at up to 165°C, e.g., automotive applications.

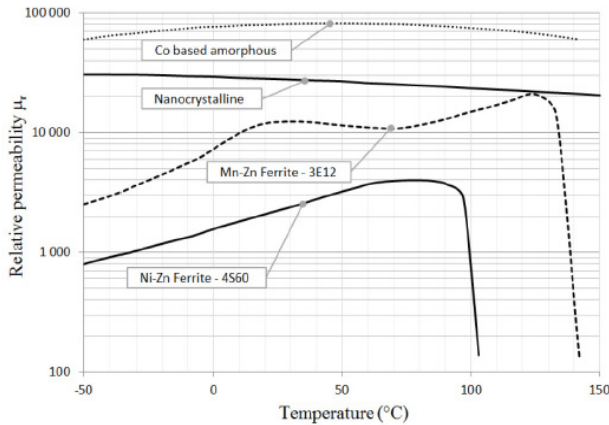


Figure 8: Permeability vs Temperature for Various Magnetic Materials [10]

## Cost

Cost is always going to be a key factor in deciding which material to use. Tradeoffs must be considered for performance vs cost. A small number of ferromagnetic materials will be suitable for any given application. Based on the materials suitable for the specific application, the designer should choose the material that meets the target system specifications at the lowest possible cost. For low frequency (<5 kHz), high current sensing applications, SiFe is a common choice for its high saturation magnetization, relatively low coercivity, ease of manufacturing laminated cores, and low cost.

## CORE GEOMETRY

The shape of the core (circular, rectangular, etc.), inner and outer dimensions, and cross-sectional area will all influence the behavior of the core. However, the size of the air gap will dominate the gain of the design. The primary goals in the core design are as follows:

- Maintain exceptional linearity performance through the operating current range while avoiding magnetic saturation.
- Minimize outer core dimensions to reduce the mechanical footprint, cost, and weight of the solution.

- Minimize air gap to increase magnetic signal and stray field immunity, while taking care to avoid localized saturation in the core.

For high currents >200 A, it is more practical to use a busbar than a wire conductor, so this section is focused on rectangular core geometries. Using a rectangular core matches the form factor of the conductor better than a circular core and will reduce the overall mechanical footprint. The gain and saturation point of the flux concentrator is dominated by the air gap length and cross-sectional area of the core. Shape of the core, whether circular or rectangular, will have minimal impact on performance.

## Air gap and cross-sectional area

As mentioned previously, the gain of the system will be dominated by the air gap length. The amount of magnetic flux induced in the core and the coupling factor to the Hall-effect sensor is proportional to the length of the air gap. To first order, the amount of magnetic flux density in the air gap can be estimated by equation 1 which can be further simplified to equation 2.

$$B = \frac{I\mu_0}{l_g}$$

Equation 1

Where:

$B$  = magnetic flux density (T)

$l_g$  = length of air gap (m)

$\mu_0$  = permeability of free space

$I$  = busbar current (A)

$$B(G) = 12.5 \frac{I(A)}{l_g(mm)}$$

Equation 2

Second order effects, such as magnetic fringing, will also be dependent on the length of the air gap and will impact coupling factor. ANSYS Maxwell 3D software was used to simulate coupling factor vs. air gap length. Figure 9 shows how the simulated results track the calculation from equation 2 for a fixed cross-sectional area. As the air gap increases, magnetic fringing contributes to a reduction in expected coupling factor, and the first order estimation of equation 2 loses accuracy.

[10] M. Kacki, J.G. Hayes, M.S. Rylko, C.S. Sullivan "Magnetic Material Selection for EMI Filters," IEEE Energy Conversion Conference and Exhibition, Cincinnati, October 2017.

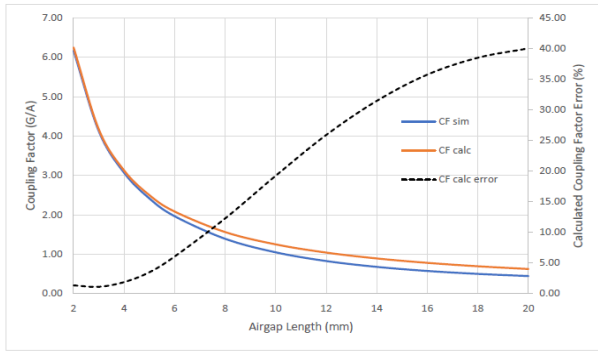


Figure 9: Coupling Factor vs. Air Gap

In general, a smaller air gap is desirable for maximizing flux density, coupling factor, and stray field rejection while minimizing the amount of magnetic fringing which could result in a reduction in coupling factor to the sensor as well as cross coupling into other sensitive circuitry.

There are also practical limitations to consider when sizing the air gap. While a smaller air gap is desirable for an increased magnetic field at the Hall-effect sensor, there is a limit to how much field a sensor can handle. For example, the maximum operating field for the ACS70310 is  $\pm 3000$  G. Figure 10 illustrates the impact air gap length has on magnetic flux density and coupling factor. The thickened section of the field strength traces indicates the linear region, defined here as the point at which a 1% linearity error is realized.

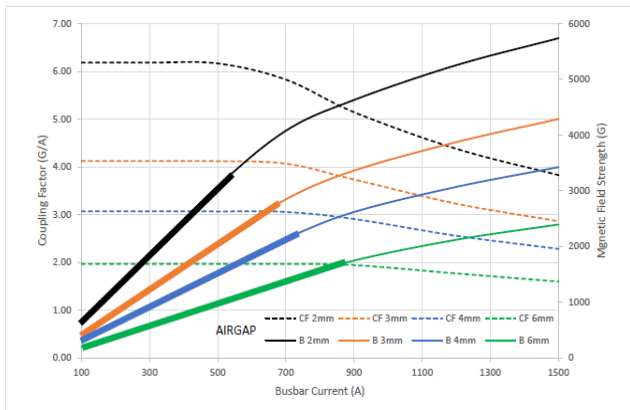


Figure 10: Magnetic Field Strength and Coupling Factor vs. Busbar Current and Air Gap Length

Core linearity is further illustrated in the coupling factor plot of Figure 11 which shows the change in coupling factor as a function of busbar current and air gap. The point at which the transfer function begins to roll off indicates the point where the core begins to saturate. Figure 12 shows a magnitude plot of the magnetic field present in the core with a 3 mm air gap, 36 mm<sup>2</sup> cross-sectional area, and 700 A of current flowing through the

busbar. It is clear from Figure 12 that localized saturation is beginning to occur in the section of the core opposite the air gap. A flux concentrator must allow for a linear current measurement over the specified current range. This requires a design which does not go into saturation under normal operating conditions and provides some margin for overcurrent conditions.

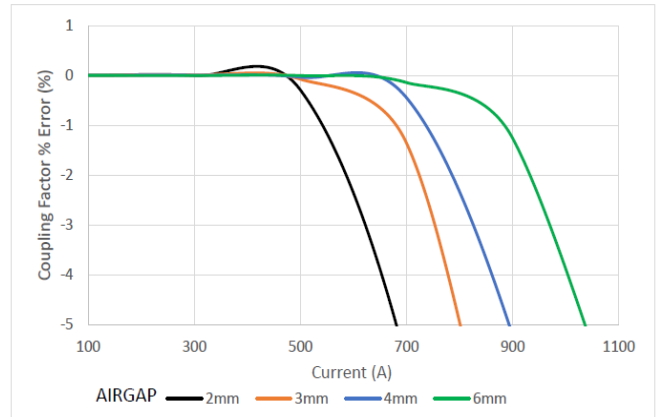


Figure 11: Coupling Factor Percentage Error vs. Busbar Current

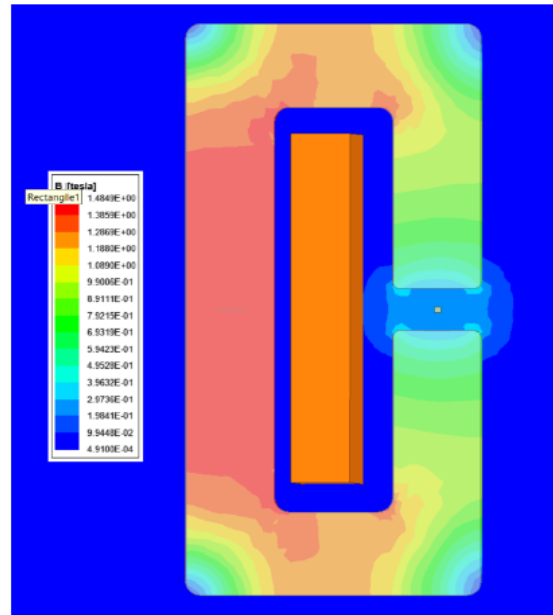


Figure 12: Magnetic Field Magnitude in Core

The cross-sectional area of the core can also be manipulated to avoid localized saturation at a given air gap length and current level. The magnetic flux in the core will be dictated by the dimensions of the air gap, however, the magnetic flux density in the core will have an inverse relationship to the cross-sectional area. So an increase in cross-sectional area will result in a reduced magnetic flux density in the core and an increased saturation current level. For example, Figure 10 through Figure 12 show

data from a SiFe core with a cross-sectional area of 36 mm<sup>2</sup>. At an air gap length of 4 mm this core begins to saturate and become non-linear at ~700 A. Increasing the cross-sectional area of the core to 60 mm<sup>2</sup> increases the linear operating range of this system to over ~900 A. Figure 13 shows the impact of cross-sectional area on core saturation.

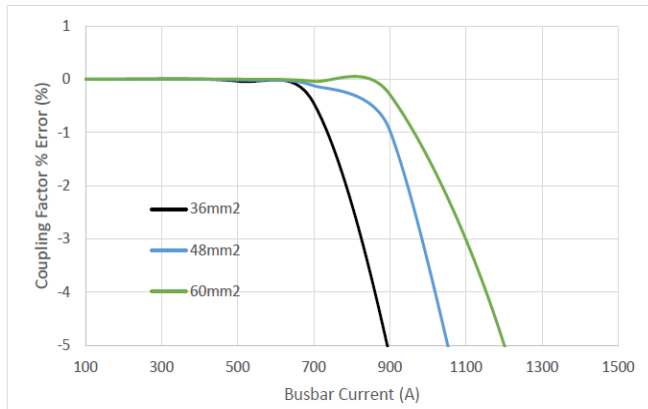


Figure 13: Change in Coupling Factor vs. Busbar Current and Core Cross-Sectional Area

Additionally, increasing the cross-sectional area of the core, particularly at the air gap, has the benefit of reducing fringing and increasing coupling factor at large air gap lengths. For example, Figure 9 shows that the simulated coupling factor is degraded by ~20% from the expected value at an air gap length of 10 mm with a cross-sectional area of 36 mm<sup>2</sup>. Figure 14 illustrates the relationship between coupling factor degradation versus cross-sectional area at the air gap. The plot shows the impact of increasing the cross-sectional area by just increasing one side of the area versus increasing both sides. Clearly, increasing both sides of the air gap proportionally yields better results. Of course, a larger cross-section will result in a heavier, more expensive core that will require a larger mechanical footprint.

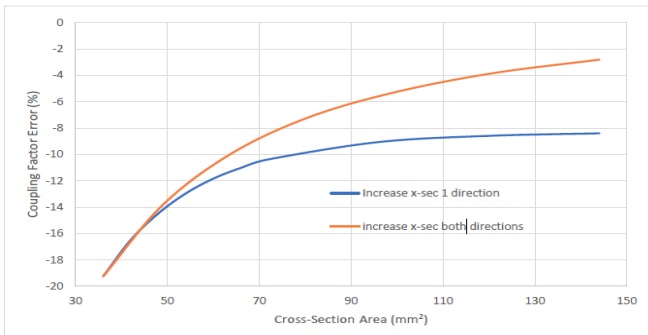


Figure 14: Coupling Factor Error vs. Air Gap Cross-Sectional Area

## ERROR SOURCES

Mechanical and manufacturing tolerances will introduce various error sources into the system. These error sources include, but are not limited to:

- Air gap length variation
- Location of sensor within air gap
- Tilt of sensor within air gap
- Location of busbar with respect to core
- Variation in lamination thickness and stacking factor of laminated cores

Assuming standard manufacturing tolerances, each of these will have small to negligible impact on system performance. Additionally, these error sources are fixed and will not vary over time so they can easily be calibrated out at end of line calibration.

The Hall-effect sensor chosen will also introduce measurement errors, specifically offset and sensitivity error. The nominal errors will be calibrated out at end of line calibration; however, any temperature drift must be accounted for when selecting a sensor. Any sensor datasheet will specify the amount of offset and sensitivity drift that can be expected.

## DESIGN EXAMPLE

The design example is based on the following system requirements:

1. Max Continuous AC current: 200 A<sub>RMS</sub> (280 A<sub>PK</sub>)
2. Max AC current, 2s: 500 A<sub>RMS</sub>
3. Measurement range: ±800 A<sub>PK</sub>
4. Current Frequency: 1 kHz
5. ±2 V full-scale ADC input range
6. ±5% measurement error
7. -40°C to 85°C

A 25 mm × 4 mm busbar is designed to handle 200 A<sub>RMS</sub> of continuous AC current. For a low-cost, low-frequency design, requiring good accuracy and high magnetic flux density, a SiFe core is chosen. Based on simulation, a core is specified with an air gap of 4 mm in length for a 3.1G/A coupling factor. A 48 mm<sup>2</sup> cross-section is chosen for the top, bottom, and gapped sections of the core while 64 mm<sup>2</sup> cross-sectional area is chosen for the back length of the core to prevent localized saturation up to ±1000 A. The core is fabricated with 0.35 mm thick laminations and a stacking factor of 0.95 to ensure flat gain and <1° of phase shift at 1 kHz. Ultimately, the core design would need to be manufactured and tested to validate simulation results. Figure 15 shows the core and busbar dimensions. Figure 16 shows simulated coupling factor error and magnetic field sensed at the air gap of the core.

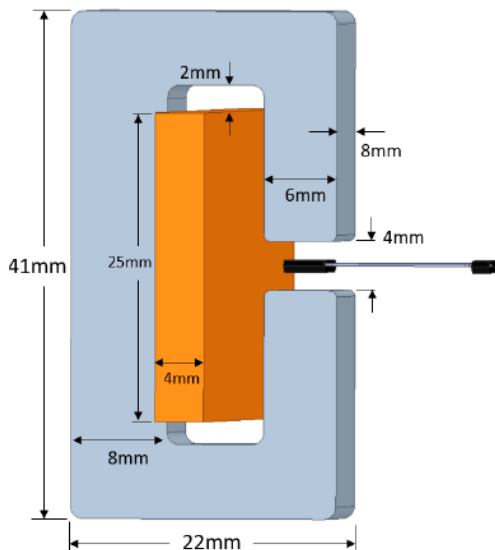


Figure 15: Example Core Design to Meet Stated Specifications

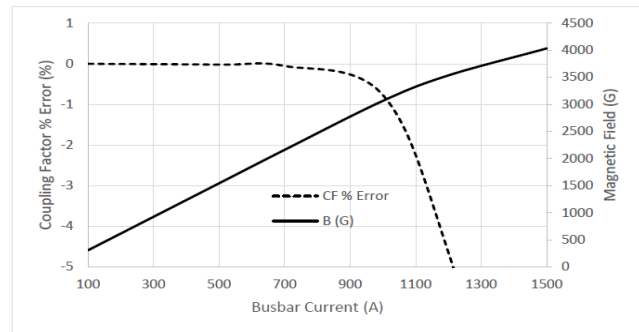


Figure 16: Coupling Factor Error and Magnetic Field vs. Busbar Current

The Allegro [ACS70310](#)<sup>[11]</sup> is chosen as the sensor for its high precision, programmable sensitivity, and performance over temperature. Considering the ACS70310 offset and sensitivity errors in addition to SiFe core hysteresis of ±2 A, this design will be able to achieve ±5% accuracy.

With a coupling factor of 3.1 G/A and a measurement range of ±800 A the core will produce ± 2480 G. To use the full dynamic range of the ±2 V ADC input range, the ACS70310 sensitivity is programmed to 0.81 mV/G.

## CONCLUSION

As system operating currents extend beyond the capabilities of shunt-based solutions and current sensors with integrated conductors, magnetic flux concentrators coupled with Hall-effect sensors provide a robust, low-cost solution for high current measurements. Based on the system operating parameters, required measurement accuracy, and cost targets, considerations must be given to the core material used, core geometry implications, and Hall-Effect sensor performance characteristics.

When selecting a core material, the magnetic hysteresis, saturation flux density, electrical conductivity, and temperature stability must be optimized for the target system specifications. The air gap length and cross-sectional area of the core geometry will dictate the coupling factor of the core design and its ability to avoid saturation. Finally, a Hall-effect sensor with adequate sensitivity, offset, and linearity performance over the specified temperature range must be chosen. Bench results must be taken to validate simulations and design iterations may be required to get the desired performance.

[11] "ACS70310 and ACS70311: 240kHz, Highest Accuracy Programmable Linear Sensor IC with Reverse Battery Protection for Core-Based Current Sensing," Allegro MicroSystems, accessed August 6, 2021, <https://www.allegromicro.com/en/products/sense/current-sensor-ics/sip-package-zero-to-thousand-amp-sensor-ics/acs70310>

## REFERENCES

1. Latham, Alexander, Scott Milne. "DC and Transient Current Capability/Fuse Characteristics of Surface Mount Current Sensor ICs." Accessed August 6, 2021. <https://www.allegromicro.com/en/insights-and-innovations/technical-documents/hall-effect-sensor-ic-publications/dc-and-transient-current-capability-fuse-characteristics>
2. Shorman, Evan, Caleb Mattson, Shaun Milano. "DC Current Capability and Fuse Characteristics of Current Sensor ICs with 50 to 200 A Measurement Capability." Accessed August 6, 2021. <https://www.allegromicro.com/en/insights-and-innovations/technical-documents/hall-effect-sensor-ic-publications/dc-current-capability-fuse-characteristics-current-sensor-ics-50-200-a>
3. S. Tumanski. 23 Jun 2011, Magnetic Materials from: Handbook of Magnetic Measurements CRC Press
4. Vuillermet, Yannick, Loïc Messier. "Ferromagnetic Concentrator Cores." Accessed August 6, 2021. <https://www.allegromicro.com/en/insights-and-innovations/technical-documents/hall-effect-sensor-ic-publications/hysteresis-mitigation-in-current-sensor-ics-using-ferromagnetic-cores>
5. J.O. Aibangbee, O. Onohaebi, "Ferromagnetic Materials Characteristics: Their Application in Magnetic Cores design Using Hysteresis Loop Measurements", American Journal of Engineering Research, Volume-7, Issue-7, pp-113-119
6. El Bacha, Georges, Shaun Milano, Jeff Viola. "Hysteresis Mitigation in Current Sensor ICs Using Ferromagnetic Cores." Accessed August 6, 2021. <https://www.allegromicro.com/en/insights-and-innovations/technical-documents/hall-effect-sensor-ic-publications/hysteresis-mitigation-in-current-sensor-ics-using-ferromagnetic-cores>
7. Vuillermet, Yannick. "High-Current Measurement with Allegro Current Sensor IC and Ferromagnetic Core: Impact of Eddy Currents." Accessed August 6, 2021. [https://www.allegromicro.com/en/insights-and-innovations/technical-documents/hall-effect-sensor-ic-publications/an296162\\_a1367\\_current-sensor-eddy-current-core](https://www.allegromicro.com/en/insights-and-innovations/technical-documents/hall-effect-sensor-ic-publications/an296162_a1367_current-sensor-eddy-current-core)
8. Marcin Kacki, Marek S. Rylko, John G. Hayes, Charles R. Sullivan "Magnetic Material Selection for EMI Filters", IEEE Energy Conversion Conference and Exhibition, Cincinnati, October 2017.
9. Allegro MicroSystems. "ACS70310 and ACS70311: 240kHz, Highest Accuracy Programmable Linear Sensor IC with Reverse Battery Protection for Core-Based Current Sensing." Accessed August 6, 2021. <https://www.allegromicro.com/en/products/sense/current-sensor-ics/sip-package-zero-to-thousand-amp-sensor-ics/acs70310>

*Revision History*

| Number | Date            | Description     | Responsibility |
|--------|-----------------|-----------------|----------------|
| -      | August 30, 2021 | Initial release | Kevin Buckley  |

Copyright 2021, Allegro MicroSystems.

The information contained in this document does not constitute any representation, warranty, assurance, guaranty, or inducement by Allegro to the customer with respect to the subject matter of this document. The information being provided does not guarantee that a process based on this information will be reliable, or that Allegro has explored all of the possible failure modes. It is the customer's responsibility to do sufficient qualification testing of the final product to ensure that it is reliable and meets all design requirements.

Copies of this document are considered uncontrolled documents.